ACCELERATION OF ENERGETIC PARTICLES WHICH ACCOMPANY CORONAL MASS EJECTIONS

Donald V. Reames

NASA Goddard Space Flight Center, Greenbelt, MD

ABSTRACT

During the last few years it has become clear that the major solar particle events seen at Earth are causally associated with coronal mass ejections (CMEs) and not with solar flares. Particles are accelerated from the ambient plasma of the corona and solar wind by the shock wave that expands ahead of a large CME, filling the heliosphere with particles over a wide longitude range and continuing the acceleration far beyond the orbit of earth. The average element abundances of the accelerated ions reflect those of the solar corona and their ionization states (e.g. Fe^{+14}) are similar to those of the solar wind and typical of a coronal plasma temperature of ~2 MK. The lack of evidence of heating suggests that the ions cannot come from a flare or field reconnection region where temperatures reach ~30 MK. Large proton events also accompany disappearing filament events with no impulsive flare present.

In contrast, however, we also see ions that are accelerated in impulsive flares. These are the ^{3}He-rich events with 1000-fold enhancements in the $^3He/^4He$ produced by resonant wave-particle interactions in the flare plasma. Heavy elements are also enhanced and are highly ionized in these events (Fe^{+20}). The events are only seen when the observer is magnetically well connected to the flare. A few large impulsive-flare events have been observed, generally in conjunction with gamma-ray events. However, in ~90% of the large events, including ground-level events (GLEs), nearly all of the ion acceleration occurs at CME-driven shocks, not in the impulsive flare.

In the large CME related events, the particle time profiles depend strongly on the CME longitude relative to the observer. The highest intensities occur when the observer is connected to the nose of shock ahead of the CME. For western events this occurs early when the CME is near the Sun and for eastern events it occurs when the CME is well out beyond the observer. Near central meridian we see flat time profiles early, because of flux limiting near the shock, then intensities rise at the shock. Immediately behind the shock are bi-directional streaming events in the ions, probably because of the magnetic field geometry in that region. Farther behind the shock the particle intensities are nearly identical over a longitude interval as large as ~180° and they decline for many days in the expanding volume behind the CME.

For the highest energy ions, acceleration does not continue as far from the Sun because these particles are less efficiently contained when the plasma expands as R^{-2}. For protons from ~100 MeV to >20 GeV, peak acceleration occurs when the shock at the leading edge of the CME is 6-10 solar radii from the Sun.

1. INTRODUCTION

If we had just seen coronal mass ejections (CMEs) driving huge shock waves through the corona into interplanetary space *before* we observed the first solar energetic particles (SEPs), the history of SEP events might have been a great deal simpler. Unfortunately, the first clear evidence of energetic particles from the sun came in the events of February and March 1942 (Ref. 4), some 30 years before CMEs were first observed. This left a 30-year information vacuum in which the only candidate source with sufficient energy to accelerate particles was the solar flare. Despite the rather poor association between the large SEP events and flares, there seemed little alternative to accepting "the solar flare myth" (Ref. 5), that particle acceleration occurred in spatial and temporal conjunction with solar flares.

Even when flares did occur in conjunction with SEPs, it was not so easy to understand why the particle events lasted for days, much longer than flares, and how the particles could be seen at longitudes of 90° or more from the flare site. This problem was solved by the *ad hoc* proposal that the particles somehow managed to diffuse across magnetic field lines in the corona and out into interplanetary space. An entire generation of graduate students was raised on the dogma of diffusion models; all they had to do was adjust the numerous parameters of these models to 'explain' the intensity-time profile of the protons in an event.

Evidence that led to the demise of this flare-dominated paradigm for major SEP events came from several avenues.

1) CMEs were observed and 96% of the large SEP events were found to have associated CMEs (Ref. 12). Large SEP events were also associated with disappearing filament events where there was no impulsive flare (Ref. 11).

2) Element and isotope observations provided a signature of those particles that *were* associated with impulsive flares (Refs 33, 32, 30). The electron-rich, ^{3}He-rich, Fe-rich particles from impulsive events were clearly distinguished from average coronal abundances in the CME-associated gradual events (Refs. 26, 28, 31).

3) Observation of the ionization states of the energetic particles provided information on the temperature of the source plasma (Refs. 17, 18). In the gradual events the particles had the similar ionization states to those in the solar wind (*e.g.* the mean charge of Fe was 14.9±0.09), thus they showed no evidence of heating by the flare. In contrast, ions up to Si were fully ionized and Fe had charge 20.5±1.2 in ^{3}He-rich events.

4) The impulsive (^{3}He-rich) events were *not* spread in either solar longitude or in time, suggesting that diffusion along or across field lines was not of great importance.

For the large gradual events, these observations are fully consistent with acceleration of the particles from the ambient coronal plasma by the expanding shock wave from a CME. Particles are also accelerated in impulsive flares, but the

Proc of the Third SOHO Workshop – Solar Dynamic Phenomena and Solar Wind Consequences, held at Estes Park, Colorado, USA, 26 – 29 September 1994 (ESA SP-373, December 1994)

high intensities of streaming electrons generate waves below the proton gyrofrequency where they are resonantly absorbed by ^{3}He (Refs. 35, 19). The same electron beams that produce type III radio bursts and hard X-ray emission in impulsive flares probably also generate the plasma waves that cause the abundance enhancements.

It is interesting from a historical perspective that idea of two distinct types of acceleration, including shock acceleration of protons, was proposed, based on radio observations (Ref. 38), at about the same time as the 'coronal diffusion' models. Direct observation of interplanetary shock waves had also been made. Nevertheless, the diffusion picture continued to predominate up until the last few years.

Once we have correctly identified the source of the energetic particles in the gradual events, we can begin to use them as probes of the structure and evolution of the CME and shock as they expand outward through the interplanetary medium. The particles stream away from the shock along magnetic field lines with speeds of ≥1 AU/hr. An observer views particles accelerated at the point where his field line intercepts the shock. This point sweeps eastward with time; eventually it can scan across the entire CME structure from west to east, viewing the expanding shock first from the outside and then from the inside.

2. IMPULSIVE AND GRADUAL EVENTS

In recent years it has become possible to distinguish the particles from impulsive and gradual events using only observations of the particles themselves (Refs. 26, 28). In 1970, Hsieh and Simpson (Ref. 8) first observed particle events with large enhancements in the ^{3}He/^{4}He ratio. In the solar atmosphere or the solar wind, this ratio is 5×10^{-4}; we routinely observe ^{3}He-rich events with ^{3}He/^{4}He ≥ 1. Abundances of heavy elements such as Ne, Mg, Si and Fe are also enhanced relative to C, N and O in these events (see Ref. 31). Waves, produced by electron beams, are resonantly absorbed by ^{3}He and the heavy ions to produce these enhancements (Refs. 35, 19). Figure 1 shows the a plot of Ne/CNO *versus* Fe/CNO for impulsive (solid symbols) and gradual (triangles) events normalized to coronal abundances. The gradual events have Fe abundances that are distributed about the coronal value and Ne abundances at the coronal value. For impulsive events, Ne is elevated by an average factor of ~3 and Fe by a factor ~10. Mg and Si behave similarly to Ne. Gamma-ray line observations show that the abundances in the energetic beam inside the flare loops are the same as those in ^{3}He-rich particle events (Ref. 20). In most cases, we can clearly distinguish particles from impulsive and gradual events by their element abundances alone.

While the terms 'impulsive' and 'gradual' are taken from the X-ray time scales of the events, they could equally well refer to the intensity-time profiles of the particles. The large event beginning at W21° at 0658 UT on 1981 November 22, shown in Figure 2, is dominated by protons, has Fe/O ~ 0.1, and lasts for ~3 days. The impulsive events from W82° and W74° shown in the figure, are dominated by electrons, have Fe/O ≥ 1, and last only a few hours. The durations of the impulsive events are indeed extended because of particle scattering in interplanetary space, but only a few hours. Observation of hundreds of events like those in Figure 2 show that the abundances and the time profiles are highly correlated. Both are properties of the nature and persistence of the source, not of the corona and interplanetary medium that are common to all of the events.

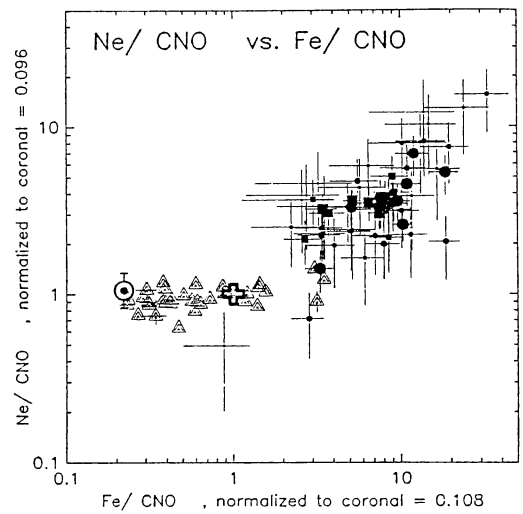

Fig. 1. The abundances of Ne and Fe relative to CNO from gradual (triangles) and impulsive (solid symbols) events, normalized to coronal abundances (Ref 31). Symbol sizes vary inversely with errors. The large cross and circle are the coronal and photospheric abundances, respectively. With few exceptions, impulsive and gradual events can be distinguished by element abundances alone.

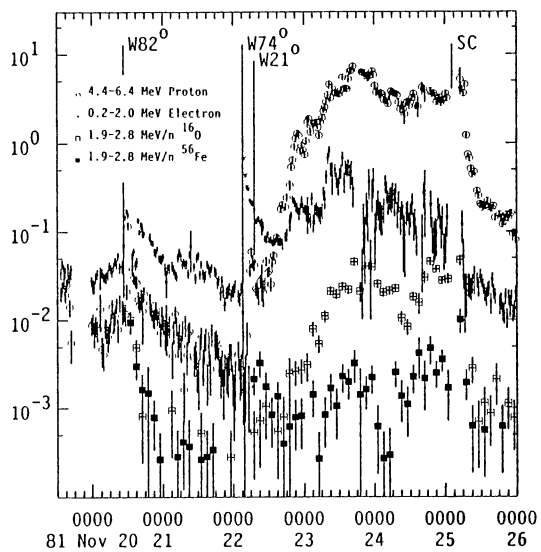

Fig. 2. Intensities of protons, electrons, O, and Fe are shown for a period during Nov., 1981 that includes two impulsive events and one gradual event. Note the obvious correlation between abundances and time scales for the two types of events. The gradual event is dominated by protons and has Fe/O ~ 0.1, while the impulsive events are electron dominated with Fe/O ≥ 1.

The longitude distribution of impulsive and gradual events is shown in Figure 3. Gradual events are also seen from

sources beyond the limbs, but such events are not included in the figure. The width of the distribution of the impulsive-flare events is ~30°, but part of this width certainly comes from the effect of solar-wind speed on the connection longitude. The intrinsic longitude interval over which an event is visible is somewhere between 5° and 20°; it is determined by the degree of 'tangling' of the field lines caused by random motion of their footpoints.

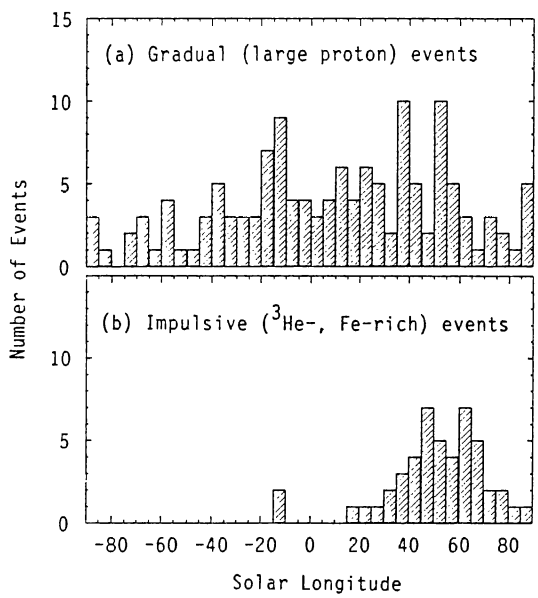

Fig. 3: Longitude distribution of gradual and impulsive events. Much of the spread in longitude for the impulsive events probably comes from variations in solar wind speed.

One of the most significant differences between gradual and impulsive events is the measured ionization states of the energetic ions, since they impose constraints on the temperature of the source plasma. The charge states of all the dominant elements are measured (Refs. 17, 18), but that of Fe is the most sensitive to temperature. In gradual events the average charge state of Fe is 14.9±0.09 (Ref. 17) with a broad distribution that is similar to the Fe charge distribution in the solar wind. These measurements are made at ~ 1 MeV/amu, however, more recent measurements of >200 MeV/amu Fe (Ref. 1) give a charge of 12.5 for 3 events in September-October 1989. These energetic particles in the gradual events do not come from material that has been heated in a flare; they represent ambient material that is accelerated from the corona and solar wind. In contrast, Fe ions in impulsive events have a mean charge of 20.5±1.2 (Refs. 17, 18) that could result either from heating to a temperature of ~20 MK or from stripping of the ions in the same intense electron beams that generate the waves that affect the abundances (Ref. 19). A histogram of the measured ionization states of Fe in impulsive and gradual events is shown in Figure 4.

Substantial effort has also been made to associate the particle events with the corresponding X-ray, optical, and radio events for both gradual (Refs. 12, 11, 3) and impulsive (*e.g.* Refs. 29, 30) events. A comparative summary of the properties of gradual and impulsive events is shown in Table 1.

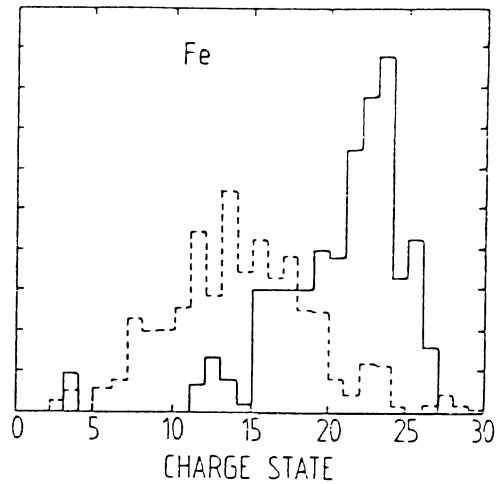

Fig. 4: Distribution of ionization states of Fe measured by Luhn *et al.* (Ref 17) in gradual (dashed line) and impulsive (solid line) events. For gradual events, the mean charge and the distribution are typical the ambient coronal plasma that has not been heated by a flare.

Table 1. Properties of Impulsive and Gradual Events

	Impulsive	Gradual
Particles:	electron-rich	proton-rich
^{3}He/^{4}He	~ 1	~ 0.0005
Fe/O	~ 1	~ 0.1
H/He	~ 10	~ 100
Q_{Fe}	~ 20	~ 14
Duration	Hours	Days
Longitude Cone	<30 deg	~180 deg
Radio Type	III, V (II)	II, IV
X-rays	Impulsive	Gradual
Coronagraph	-	CME (96%)
Solar Wind	-	IP Shock
Flares/year	~1000	~10

The event rate for impulsive events is the observed rate of ^{3}He-rich events of ~100/yr at solar maximum (Refs. 28, 31), times a factor (180°/20°) to correct for the limited longitude interval and compute the number that would be seen on the full disk. If the true longitude for an event, corrected for solar wind speed variation, were 5° or 10°, the number would be ~4000 or ~2000, respectively. The ~1000 ^{3}He-rich events may be compared with ~4000 hard X-ray bursts, ~10000 Hα flares and ~10000 type III metric radio bursts.

The ~10 gradual events/year (perhaps ~20 at solar maximum) compares with ~500 CMEs/yr at solar maximum (Ref. 36).

This low efficiency results because most CMEs do not have sufficiently high velocity, relative to the solar wind, to produce the strong shock required for particle acceleration.

2. PARTICLE ACCELERATION AT THE CME SHOCK

A typical signature of large gradual events, produced by CMEs near central meridian, is the flat profile of the low energy particles while the shock moves out from the Sun to the observer. A composite of such time profiles for several events is shown in Figure 5 (Ref. 27). There are two aspects of these profiles. First, they are flat and, second, they all seem to have the same limiting value of a few x 100 protons/(cm^2 sr sec MeV). Clearly the limit is not instrumental, since the intensities can subsequently rise another factor of 100 when the shock arrives.

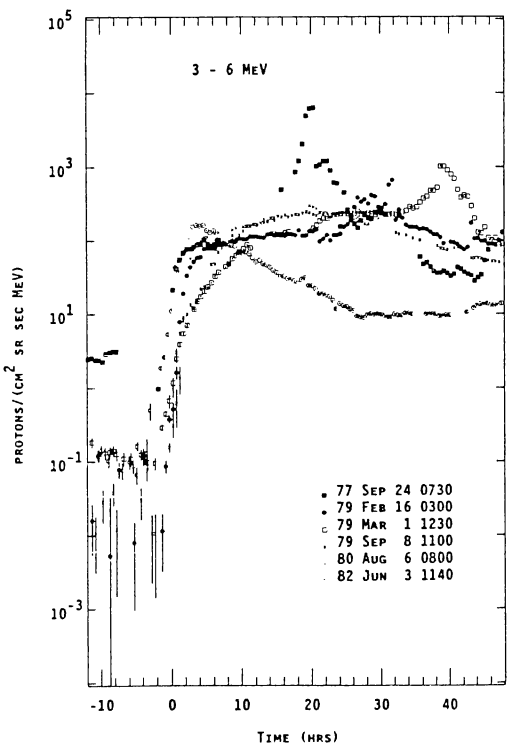

Fig. 5: A composite plot of the 3-6 MeV proton intensity for several large gradual events, showing flat profiles at an approximately constant value early in the events (Ref. 27).

A simple understanding of the flatness of the profiles comes if we consider a shock that accelerates a constant fraction of the local solar wind to the energy of observation. If the solar wind expands as $1/R^2$ and the accelerated particles from the continuous source also expand like $1/R^2$, the same intensity will be observed from acceleration near the Sun or near the Earth. Much more detailed model calculations of Lee and Ryan (Ref. 16), for example, also show such flat profiles. Thus the flat profiles result from nearly constant acceleration.

The existence of a nearly constant limiting intensity in many events may come from a breakdown of wave-particle equilibrium near the shock. As particles stream away from the shock they excite Alfvén waves. These waves scatter subsequent particles of the same energy and reduce the streaming. Each time a particle traverses the shock it gains energy. When the magnetic field is parallel to the shock normal, the particle gains energy incrementally from the change of velocity across the shock, as if it were being reflected between approaching mirrors. For oblique field angles, the particle can also gain energy by drifting in the $\mathbf{V} \times \mathbf{B}$ electric field parallel to the shock. In any case, multiple traversals of the shock are required to accelerate particles from ~1 keV of the ambient plasma to MeV or GeV of the energetic particles, so scattering by self-generated waves is essential. The theory of Lee (Ref. 15) describes the formation of an equilibrium between particles and resonant waves so that the intensities of both depend only on distance from the shock. At some distance from the shock the wave intensity is not sufficiently high to impede the particles so they can stream freely away. This results in an intensity-time profile like the one in Figure 6A. The particles that arrive first were accelerated by the shock when it was near the Sun and the intensity remains roughly constant at the saturation value until the arrival of the wave-trapping region that accompanies the shock. Historically, the wave-trapping region near the shock was called an 'energetic storm particle' or ESP event.

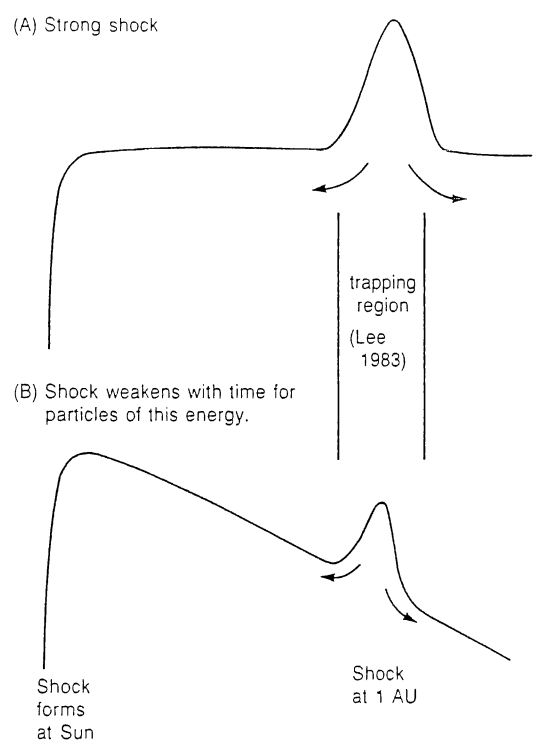

Fig. 6: Intensity *vs.* time profiles for particles where strong acceleration continues out to the observer (A) or diminishes with time (B). *All* particles are accelerated by the shock in either case. The 'ESP' bump is often absent (see text).

As the shock expands outward, the densities of both particles and resonant waves decreases approximately as $1/R^2$. Thus the particle intensity may become insufficient to generate enough resonant waves to contain the particles and continue

the particle intensity may become insufficient to generate enough resonant waves to contain the particles and continue the acceleration. An acceleration efficiency that decreases with R, hence with time, can produce an intensity-time profile like that in Figure 6B. It is also possible that the trapping structure dissipates completely before reaching the observer; in this case the 'ESP' bump is missing. This occurs especially at high energies where the particle intensities are low initially; such particles are soon unable to produce waves that resonate with them and acceleration ceases.

The saturation of particle intensities caused by self-generated waves was explored recently in detailed calculations by Ng and Reames (Ref. 22), not in the context of shock acceleration, but for any source near the Sun. Table 2 of that reference shows that as the intensity of 45 MV (~1 MeV) protons increases logarithmically near the Sun, the intensity near 1 AU flattens at a value of ~200 protons/(cm^2 sr sec MeV). The protons regulate their own intensity by self-generated waves.

At very high energies, particles are shock accelerated close to the Sun. Kahler (Ref. 10) has studied the particle intensities as a function of the distance of the leading edge of the CME from the Sun for 'ground level events' (GLEs) where particle energies are many GeV. Figure 7 shows that the acceleration of particles up to 21 GeV maximizes at 5-15 solar radii. The CME speed in the 1989 September 29 event is 1828 km/s (Ref. 10), quite adequate to drive a shock across the high corona from the event at W105° to the field line to Earth. This is also an event where 200 MeV/amu Fe had an ionization state of 12.5 (Ref. 1), indicating acceleration of ambient unheated coronal material.

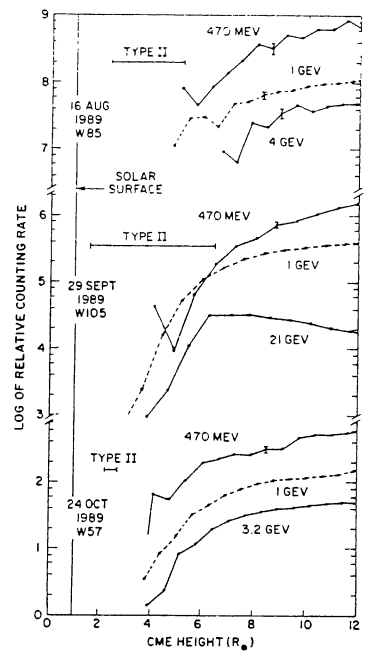

Fig. 7: Intensity *vs.* altitude of acceleration of particles of several GeV energy in GLEs (from Kahler, Ref 10).

The most dramatic influence on the appearance of particle time profiles comes from variation in the longitude of the observer's connection to the CME shock shown in Figure 8.

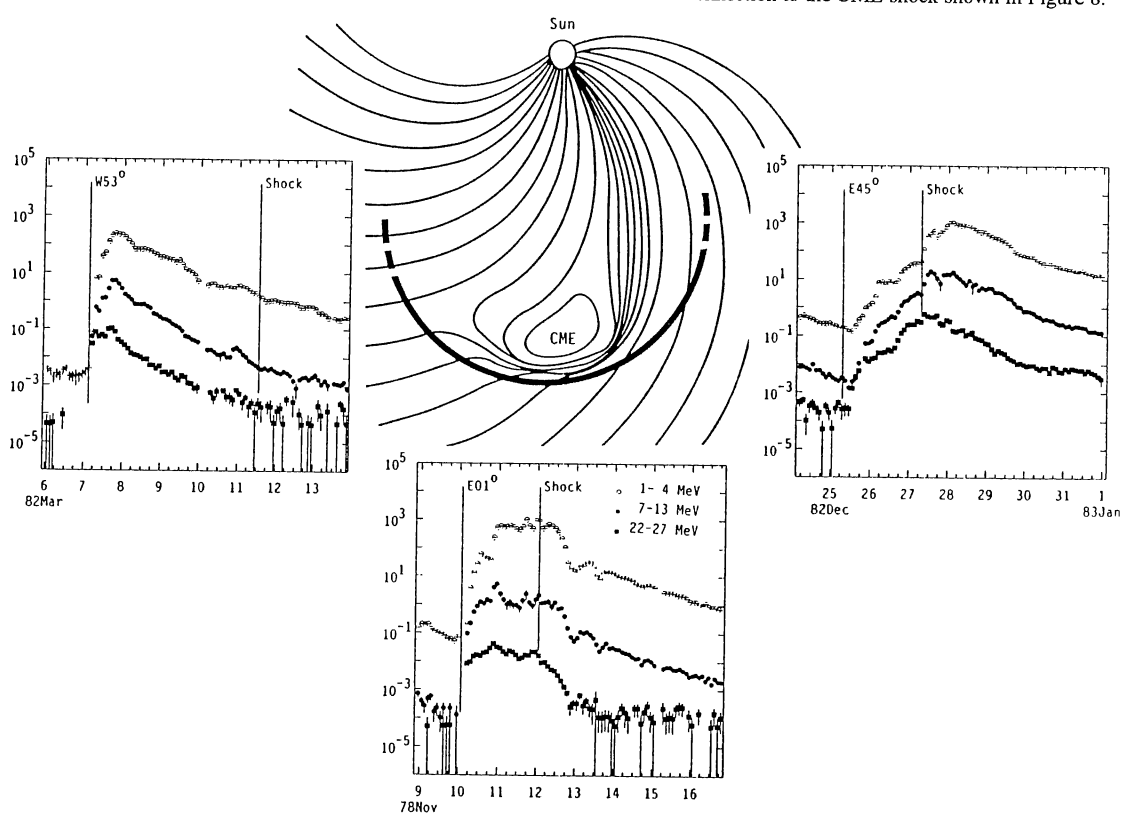

Fig. 8: Typical intensity-time profiles of protons at 3 different energies for observers viewing a CME at the 3 longitudes indicated.

An observer viewing a CME near central meridian will usually see flat intensity-time profiles as seen for the E01° event in Figure 8. The central region or 'nose' of the shock where the strongest acceleration occurs remains reasonably well connected to the observer for the time of ~2 days before the shock arrives.

The observer viewing the event at W53° in Figure 8 is extremely well connected to the nose of the shock when it is near the Sun so he sees a fast rise to high intensities early. By the time the shock passes this observer, however, he is now far around on the eastern flank of the shock (if it is seen at all) where few particles have been accelerated. Thus his profile declines rapidly with time.

The observer seeing a CME at E45° in Figure 8 may see a few particles early when the western flank of the shock begins to accelerate particles at the base of his field line in the corona. As the stronger central regions of the shock expand outward they contact field lines farther to the west while the spacecraft moves eastward, magnetically, because of solar rotation. Thus his field line scans rapidly eastward to stronger and stronger regions of the shock. For the example in Figure 8, he must pass behind the local shock to encounter field lines that connect him to the nose of the shock before the intensities reach maximum.

The profiles in Figure 8 are not different views of a single event, rather, they are 'typical' profiles observed from a single near-Earth spacecraft, IMP 8, for different CMEs. Cane, Reames and von Rosenvinge (Ref. 3) studied a sample of 235 proton events (20 years of data) grouped by the longitude of the associated flare (when one occurred). Observations of a single event with multiple spacecraft will be discussed in the next section.

3. MULTI-SPACECRAFT OBSERVATIONS

While the observations of many CME events from a single spacecraft can give the general shape of the intensity profiles as a function of longitude, the relative amplitudes of these profiles can only be determined by scanning across a single CME event with multiple spacecraft. Previous multi-spacecraft studies (*e.g.* Ref. 11) have been used primarily to study peak intensities *vs.* longitude and the detailed shapes of the profiles have not been systematically compared.

3.1. Case 1: A Typical Event

Figure 9 shows the view of a typical gradual event obtained from IMP 8 and the Helios 1 and 2 spacecraft. As shown in the figure, the event is at E58° to IMP 8 but is near central meridian to Helios 1. Helios 1 is rather poorly connected early in the event but begins to see the characteristic flattened profile at the limiting intensity at 3-6 MeV as the CME moves outward and the connection to the nose of the shock improves. The shock passes Helios 1 at the peak of the 'ESP' intensity increase as we would expect from the discussion of Figure 6A. Subsequently the intensity decreases by an order of magnitude and then begins a long slow decay. Helios 2 sees the slower intensity rise of a near eastern event at 3-6 MeV. Soon after the spacecraft passes the shock, however, it enters a region where the intensity behavior is nearly identical to that of Helios 1. IMP 8 is initially connected even farther (~110°) around on western flank of the shock where the intensities are much lower. The magnetic connection longitude improves with time until it is 58° from the peak as the shock passes Earth. On March 5, when the nose of the shock is at ~ 2 AU, IMP 8 finally encounters field lines where the low-energy intensities are similar to those the other 2 spacecraft.

Nearly all of the behavior of the low-energy particles in Figure 9 can be explained by the changing connection between the observer's field line and the shock. Particles seen by the observer are accelerated at this point. As the point sweeps eastward with time toward the nose of the shock, intensities increase. Even when the spacecraft penetrates the local shock the intersection point continues to scan eastward across the back (sunward side) of the shock, despite field distortions, until it has magnetically traversed the entire structure.

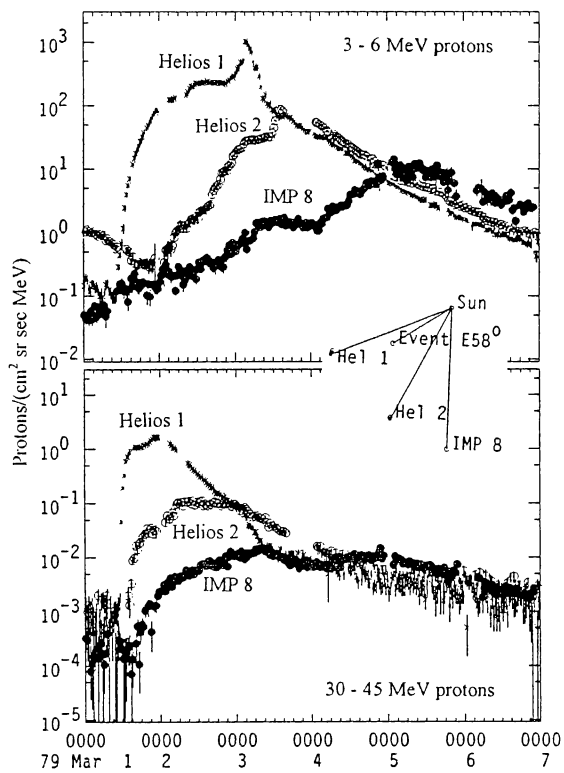

Fig. 9: Intensity *vs.* time of particles at 2 energies for a CME event observed by 3 different spacecraft in the configuration shown.

While the intensities of low-energy particles depend primarily on connection longitude, those of higher-energy particles depend upon connection convolved with radial- or time-dependent acceleration. Since the acceleration efficiency at any point on the shock decreases with time at high energies, the higher-energy profiles in Figure 9 peak earlier than the corresponding low-energy profiles.

The long slow decline of all of the profiles at all energies late in the event actually continues for 3 more days beyond the end of Figure 9. The particles are contained in a volume behind the shock that is expanding with time. However, it is not entirely clear why the 3 spacecraft separated an angle as large as 60° see intensities that differ by only a factor of ~ 2 or less. We will see that this is a common feature of large gradual events.

3.2 Case 2: Slow Acceleration?

Slowly rising time profiles like the one in Figure 10 are easily misinterpreted in two different ways. Either the particles are found to be slowly diffusing away from an advancing shock (Refs. 2, 24) or the acceleration by the shock is so inefficient and slow that it takes several days for the intensities to build up to the level observed when the shock reaches the observer (Refs. 14, 37). Both of these interpretations are based on the false assumption that the observer is privileged to remain on a single bundle of field lines watching temporal evolution. In the previous section, however, we found that the dominant effect was a changing connection point to a shock with spatially varying strength.

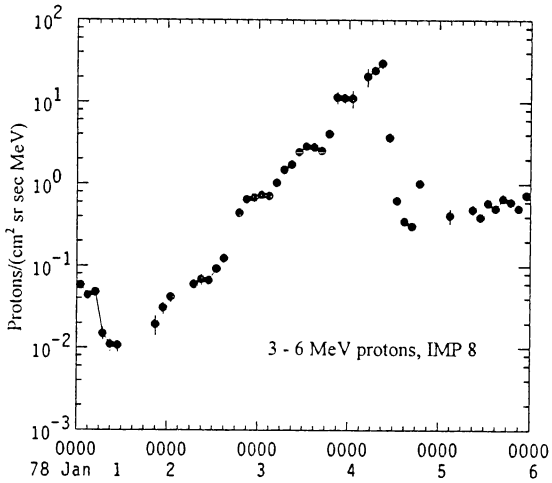

Fig. 10: An event with a gradually rising intensity that is commonly misinterpreted (see text).

Since we can not distinguish the possible origin of a single profile on a single spacecraft, we attempt a multi-spacecraft view in Figure 11. IMP 8 and the nearby Helios 2 see the same rising profile at 3 - 6 MeV. However, Helios 1, farther to the east sees a typical flat profile with a fast rise. Clearly 3 - 6 MeV protons are being accelerated quite efficiently farther to the east.

While the E6° longitude suggests that the CME is directed toward Helios 2, the particle intensities suggest it is directed toward Helios 1. This discrepancy may occur because CME longitudes cannot be measured, even when the CMEs are directly observed, because they are seen from the ecliptic plane. The longitudes quoted are *always* those of an associated *flare*. It is always possible, even likely, that the flare is not centered on the CME which has an average span of ~40°. Hence CME longitudes can have a significant error.

Returning to consider the lower panel in Figure 11, we see that the 11 - 22 MeV protons appear to be accelerated early even at IMP 8. If the shock is too weak to accelerate 3 MeV protons early, how can it accelerate the 11 MeV protons so well? In fact, if we simply look at the profiles at IMP 8 as a function of energy in Figure 12, we see that this "weak" shock accelerates particles of over 100 MeV rather easily.

A more correct interpretation of the IMP 8 data is that the hard spectrum at low intensity is observed early from the western flank of the shock. When the shock arrives, IMP 8 is well connected, but the shock, now out at 1 AU can no longer accelerate high-energy particles as efficiently, so the spectrum has softened.

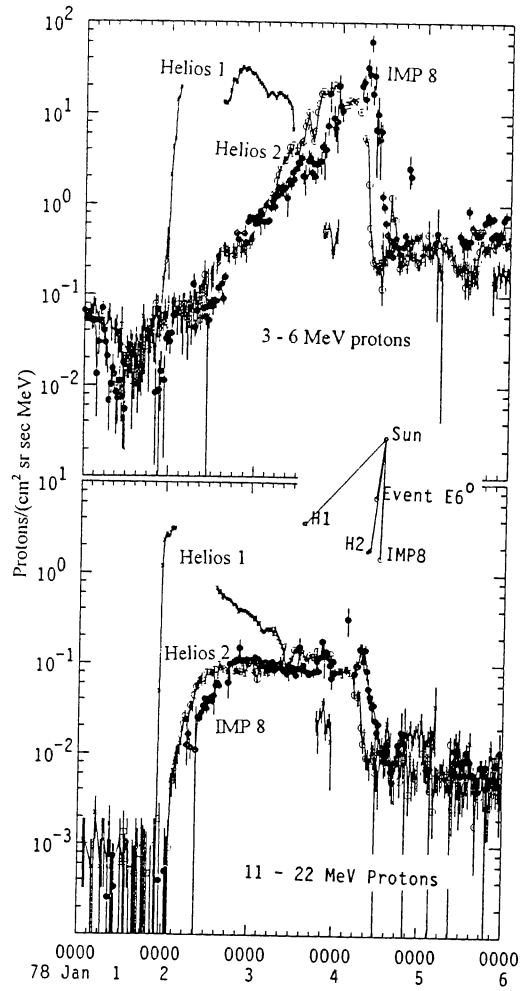

Fig. 11: Multi-spacecraft view of the event in Figure 10.

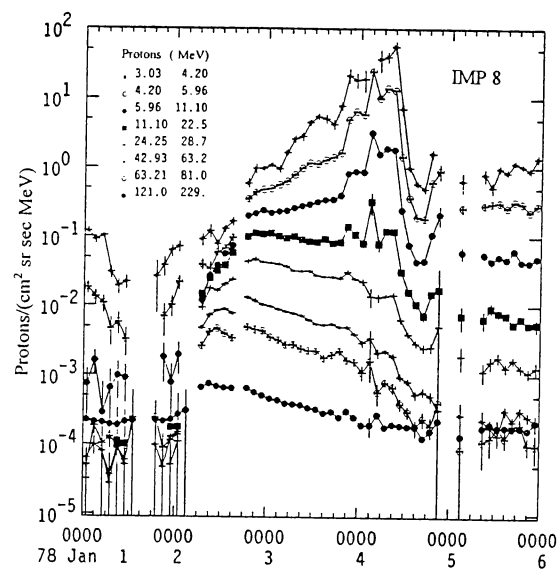

Fig. 12: High-energy profiles show strong shock acceleration early in the event of Figure 10.

3.3 Case 3: Wide Longitude Extent

The event shown in Figure 13 behaves similarly to those described above. IMP 8 is extremely well connected to the event at W50° so intensities rise rapidly. Helios 1 and 2 show slower increases appropriate to an eastern event. Behind the shock all 3 spacecraft see nearly identical intensities for several days. Note, however, that the 3 spacecraft span an opening angle of nearly 180°.

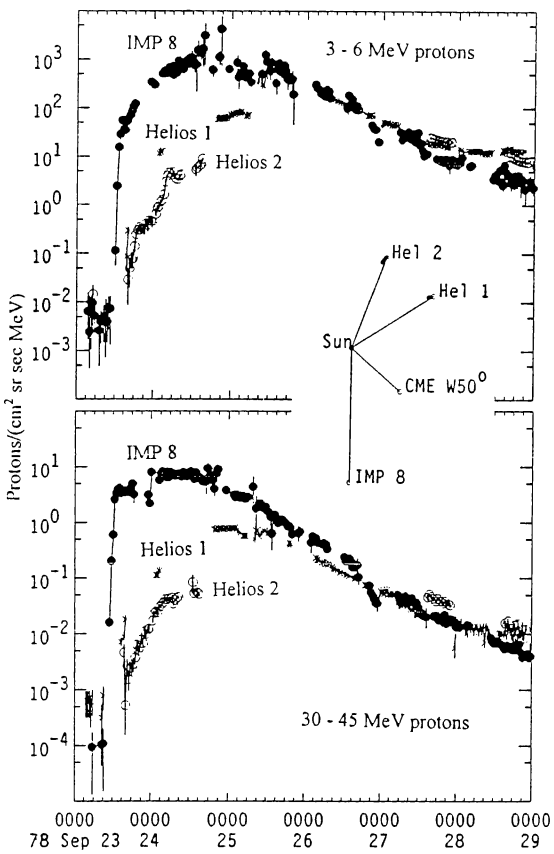

Fig. 13: Intensity *vs.* time of particles at 2 energies for a CME event observed by 3 widely separated spacecraft in the configuration shown.

3.4 Case 4: Delayed Proton Events

Many of the events we observe have relatively well- behaved intensity-time profiles that obey the rules that we have defined above. However, in some events, passage of the spacecraft from one plasma regime to another can lead to sudden changes in the connection between the observer and the shock. An example is shown in Figure 14. The event at E36° is seen as a typical western event by Helios 1, with a fast rise and smooth rapid decay. Because of relatively slow solar wind speed, Helios 2 is magnetically connected much farther around to the west than its position would imply. Thus, a very slow rise in intensity is seen initially at Helios 2 since it is poorly connected to the shock. As the high-speed wind overtakes the spacecraft it is suddenly connected to the same regime as Helios 1 and measures an identical particle intensity. If we did not have the Helios 1 data, we might assume that a new injection of particles had occurred at about 0600 UT on December 21. Not only is there no event seen at the Sun, but the identical intensities of the two spacecraft strongly suggest that Helios 2 has merely joined in the observance of the event of December 19 2156 UT that is already in progress.

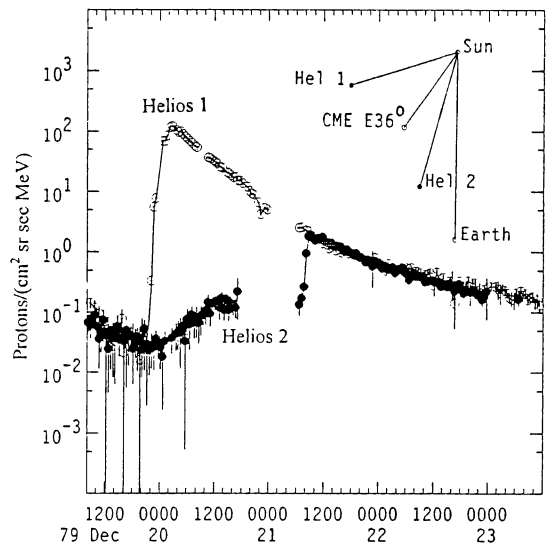

Fig. 14: A sudden connection of Helios 2 to an event already in progress appears as a 'delayed proton event'.

The classic delayed proton event is the huge particle increase observed at Earth on 1979 June 6 from an E14° event at 0514 UT on June 5. The event begins to rise after a sector boundary crossing near 1200 UT on June 6; it peaks late in the same day as the solar wind speed increases from 300 to 600 km/s at shock passage. Unfortunately there is no spacecraft farther to the east to confirm that the event is already in progress in this case.

4. THE INTERPLANETARY CME: BI-DIRECTIONAL PROTON EVENTS

Energetic particles are sensitive to the geometry and topology of the interplanetary magnetic fields. In converging fields they mirror and in diverging fields they are focused into alignment with the field. When scattering is minimal they trace out the field line on which they are accelerated. The suggestion that 'magnetic bottles' (which could contain or exclude particles) are ejected from the Sun was made 40 years ago (Refs. 21, 5). Bi-directionally streaming protons and electrons were subsequently observed (Refs. 25. 23) and were interpreted in terms of the structure of the ejected field. Controversy over the field topology has persisted to the present time. This controversy has been joined by Kahler who has provided a complete review of the subject at this conference.

While bi-directional proton events are seen about 12% of the time (Ref. 34) at solar maximum; not all of them are clearly associated with CMEs. However, a clear example of a bi-directional event is shown in Figure 15. Following the usual flat intensity (A0) profile and the passage of the shock (near November 12 0000), the particle intensity decreases by a factor of ~50. In this latter region, the particle angular distribution in the lower panel of Figure 15 shows an 8-hr

period, beginning near November 12 1800, with two oppositely directed maxima that are aligned with the magnetic field. Coefficients of the Legendre polynomial expansion in the upper panel show A2>A1 during the bi-directional period.

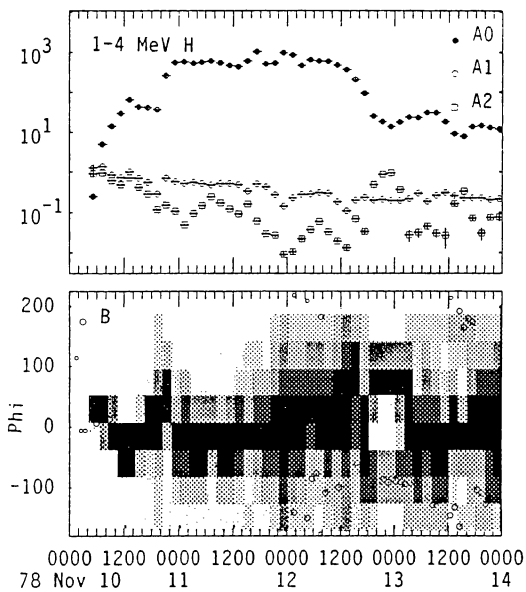

Fig. 15: Intensity (A0) and Legendre polynomial coefficients A1 and A2 are shown in the upper panel. Sectored 1-4 MeV proton intensity is shown in gray-scale as a function of azimuth angle and time in the lower panel. Circles in the lower panel show the azimuth of the magnetic field, B.

4. CONCLUSIONS

We have made substantial progress in recent years in understanding the characteristics of solar energetic particles and their relation to the physical mechanisms of acceleration. Thus:

1) We can *easily* distinguish particles accelerated in impulsive flares from those accelerated at CME-driven shocks.

2) Energetic particles in gradual events are accelerated at the point of intersection of the observer's magnetic field line with the distant CME shock. This point sweeps eastward across the entire shock structure as a function of time.

3) Regions of bi-directional ion streaming behind the shock are frequently associated with magnetic structures in the ejecta.

4) The uniform intensities in the expanding region far behind the shock are a newly identified feature that may further define the magnetic connectivity of the fields drawn out by the CME.

One consequence of knowing of the origin of the particles is that our understanding of interplanetary particle transport has changed. Realizing that the extended time profiles come from continuous acceleration, not diffusion, allows us to make a self-consistent description of the transport of the particles from both impulsive and gradual events. The parallel scattering mean free path ranges between ~0.2 and 2 AU in this picture. Unfortunately, it is not usually possible to determine particle scattering from measured field fluctuations. Magnetic power spectra are affected by spatial discontinuities convected past the observer that the particles can not see.

Historically, we have made a lot of mistakes in our understanding of SEP events, principally because we only examined a single particle species, protons, in a limited energy region at a single point in space. The advancement in our understanding has come from the study of element abundances and ionization states, from multiple spacecraft, and from careful correlations of the particle observations with radio, optical, X-ray and gamma-ray observations in same events. Of course, those who continue to study only protons or only GLEs are likely to continue to draw the same wrong conclusions.

We have just begun to study the relationship between energetic particles and CMEs. Many features of the particle behavior and the structure and evolution of CMEs remain unclear. We can not recognize the effects of CME size and shape on the particles, we can not resolve the effects of the coronal and interplanetary portions of the shock, and we do not understand the magnetic topology in and behind the CME. Perhaps particle observations can now contribute as much to the understanding of CMEs as the observation of CMEs has contributed to the understanding of energetic particles.

Acknowledgments

The multi-spacecraft studies in this review involve work in progress in collaboration with Louis M. Barbier and Chee K. Ng who have provided invaluable assistance and many enjoyable and productive discussions during the course of this work.

REFERENCES

1. Adams, J. H., Jr., Beahm, L. P., Boberg, P. R., Kleis, T., & Tylka, A. J., 1993, HIIS observations during the large solar energetic particle event of October 1989, *Proc. 23rd Int. Cosmic Ray Conf.* (Calgary), 3, 374.
2. Beeck, J. & Sanderson, T. R., 1989, *J. Geophys. Res.* 94, 8769.
3. Cane, H. V., Reames, D. V., & von Rosenvinge, T. T. , 1988, The role of interplanetary shocks in the longitude distribution of solar energetic particles", *J. Geophys. Res.*, 93, 9555.
4. Forbush, S. E., 1946, Three unusual cosmic-ray increases possibly due to charged particles from the Sun, *Phys. Rev.*, 70, 771.
5. Gold, T., 1955, Discussion of shock waves in rarified gasses, in *Gas Dynamics of Clsmic Clouds,* Ed. J. C van de Hulst, (North Holland: New York), p105.
6. Gosling, J. T, 1993., The solar flare myth, *J. Geophys. Res.*, 98, 18949.
7. Gosling, J. T., Hildner, E., MacQueen, R. M., Munro, R. H., Poland, A. I., & Ross, C. L., Mass ejections from the Sun: A view from Skylab, *J. Geophys. Res.*, 79, 4581, 1974.

8. Hsieh, K. C., & Simpson, J. A. 1970, The relative abundances and energy spectra of ^{3}He and ^{4}He from solar flares, *Astrophys. J. (Letters),* 162, L191.
9. Kahler, S.W. 1992, Solar flares and coronal mass ejections, *Ann. Rev. Astr. Ap.* 30, 113.
10. Kahler, S. W., 1994, Injection profiles of solar energetic particles as functions of coronal mass ejection heights, *Astrophys. J.*, 428, 837.
11. Kahler, S. W., Cliver, E. W., Cane, H. V., McGuire, R. E., Stone, R. G., & Sheeley, N. R. 1986, Solar filament eruptions and energetic particle events, *Astrophys. J.* 302, 504.
12. Kahler, S. W., Sheeley, N. R., Jr., Howard, R. A., Koomen, M. J., Michels, D. J., McGuire R. E., von Rosenvinge, T. T., & Reames, D. V. 1984, Associations between coronal mass ejections and solar energetic proton events, *J. Geophys. Res.* 89, 9683.
13. Kallenrode, M. B., Cliver, E. W., & Wibberenz 1992, Composition and azimuthal spread of solar energetic particles from impulsive and gradual flares, *Astrophys. J.*, 391, 370.
14. Kallenrode, M. B. 1994, Particle Acceleration at interplanetary shocks - proton observations from a few ten keV to some ten MeV., paper D2.1-046, COSPAR 94, *Adv. Space Res.*, to be published.
15. Lee, M. A., 1983, Coupled hydromagnetic wave excitation and ion acceleration at interplanetary traveling shocks, *J. Geophys. Res.*, 88, 6109.
16. Lee, M. A., & Ryan, J. M. 1986, Time-dependent coronal shock acceleration of energetic solar flare particles, *Astrophys. J.* 303, 829.
17. Luhn, A., Klecker B., Hovestadt, D., & Mobius,E. 1987, The mean ionic charge of silicon in ^{3}He-rich solar flares, *Astrophys. J.*, 317, 951.
18. Luhn, A., *et al.* 1985, The mean ionic charge of N, Ne, Mg, Si, an S in solar energetic particle events, *Proc. 19th Internat. Cosmic-Ray Conf.*, (La Jolla) 4, 241.
19. Miller, J.A. & Vinas, A. F. 1993, Ion acceleration and abundance enhancements by electron beam instabilities in impulsive solar flares, *Astrophys. J.*, 412, 386.
20. Murphy, R. J.,. Ramaty, R,. Kozlovsky, B, & Reames, D. V., 1991, Solar abundances from gamma-ray spectroscopy: comparisons with energetic particles and photospheric abundances *Astrophys. J.*, 371, 793.
21. Morrison, P., 1954, *Phys. Rev.* 95, 641.
22. Ng, C. K., & Reames, D. V., 1994, Focused interplanetary transport of ~1 MeV solar energetic protons through self-generated Alfvén waves, *Astrophys. J.* 424, 1032.
23. Palmer, I. D., Allum, F. R., & Singer, S., 1978, Bidirectional anisotropies in solar cosmic ray events: Evidence for magnetic bottles, *J. Geophys. Res.*83, 75.
24. Quenby, J. J., Lim, T. L., Drolias, B., Keppler, E., & Frañz, M., Diffusive shock acceleration and the November 1991 event: particle diffusion mean free paths as observed from ULYSSES, , *Proc. 23rd Internat. Cosmic-Ray Conf.*, (Calgary) 30, 270.
25. Rao, U. R., McCracken, K. G., & Bukata, R. P. 1967, Cosmic ray propagation processes, 2, The energetic storm particle event, *J. Geophys. Res.* 72, 4325.
26. Reames, D. V. , 1990a, Energetic particles from impulsive solar flares, *Astrophys. J. Suppl.*, 73, 235.
27. Reames, D. V. , 1990b, Acceleration of energetic particles by shock waves from large solar flares, *Astrophys. J. (Letters),* 358, L63.
28. Reames, D. V. 1993, Non-thermal particles in the interplanetary medium, *Adv. Space Res.*, 13 (No. 9), 331.
29. Reames, D. V., Cane, H. V., & von Rosenvinge, T. T. , 1990, Energetic particle abundances in solar electron events, *Astrophys. J.*, 357, 259.
30. Reames, D. V., Dennis, B. R., Stone R. G., & Lin, R. P. 1988, X-ray and radio properties of solar ^{3}He-rich events, *Astrophys. J.* 327, 998.
31. Reames, D. V., Meyer, J. P. & von Rosenvinge, T. T. 1994, Energetic-particle abundances in impulsive solar-flare events, *Astrophys. J. Suppl.*, 90, 649, 1994.
32. Reames, D. V. & Stone, R. G. 1986, The identification of solar ^{3}He-rich events and the study of particle acceleration at the Sun, *Astrophys. J.* 308, 902.
33. Reames, D. V., von Rosenvinge, T. T. & Lin, R. P. 1985, Soles ^{3}He-rich events and Nonrelativistic Electron Events: A New Association, *Astrophys. J.*, 292, 716.
34. Richardson, I. G., & Reames, D. V., 1993, "Bidirectional ~1 MeV/amu ion intervals in 1973-1991 observed by the Goddard Space Flight Center instruments on IMP-8 and ISEE-3/ICE, *Astrophys. J. Suppl.* 85, 411.
35. Temerin, M. & I. Roth, I, 1992, The production of ^{3}He and heavy ion enrichments in ^{3}He-rich flares by electromagnetic hydrogen ion cyclotron waves, *Astrophys. J. (Letters)* 391, L105.
36. Webb, D. F., & Howard, R. A. 1994, *J. Geophys. Res.*, 99, 4201.
37. Wibberenz, G. & Kallenrode, M. B. 1994, Evolution of the particle injection at the propagating shock., paper D2.1-049, COSPAR 94, *Adv. Space Res.*, to be published.
38. Wild, J. P., Smerd, S. F., & Weiss, A. A., 1963, Solar bursts, *Ann. Rev. Astron. Ap.*, 1, 291.